Observation of radial equilibrium and transition to a helix of a gas-embedded Z pinch

A. E. Dangor, M. B. Favre Dominguez, S. Lee,* and E. Kahan
The Blackett Laboratory, Imperial College of Science and Technology, London SW7 2BZ, United Kingdom

(Received 4 October 1982)

A laser-initiated, gas-embedded Z pinch is operated with a preheat current which adjusts the plasma parameters by Joule heating and expansion so that when the main current is injected, the plasma core is heated under conditions of pressure balance. This results in a pinch which has a constant radius during the time of current rise. The pinch is stable during this time and thereafter undergoes a rapid transformation into a radially expanding helical structure. The growth time and wavelength of the instability is in good agreement with the theoretical predictions of the $m=1$ magnetohydrodynamic instability.

It is well known[1–3] that in a Joule-heated pinch it is necessary to have a particular rate of current rise $\dot{I}$ to maintain the pinch in radial equilibrium. In the laser-initiated, gas-embedded Z-pinch experiment reported by Jones *et al.*[4] the pinch, powered by a source with an $\dot{I}$ of 10^{12} A s^{-1}, was found to expand radially over the whole duration of the current. Using a source with an $\dot{I}$ of 5×10^{12} A s^{-1}, we have observed a similar expansion. Here we report on a laser-initiated gas-embedded pinch in which a preheat current is used to raise the temperature whilst lowering the density by expansion, so that when the main current is injected, the pinch is heated under conditions of pressure balance. The pinch maintains a constant radius during the time of current rise. No instabilities are observed during this time. At the end of the current rise, the pinch becomes transformed into a helical structure similar to that reported by Smärs.[5] The structure expands radially but does not break up catastrophically.

A schematic diagram of the apparatus is shown in Fig. 1. The 200-kV, 0.125-μF Marx bank pulse charges a 3-Ω, 50-ns coaxial water line. This is connected via a water gap, shunted by a 250-Ω resistor, to a matched 10-ns transfer line and then to the Z-pinch assembly. The pinch electrode separation is 5 cm. A pulsed ruby laser beam (1 J, full width at half maximum, 30 ns) is focused axially through a hole in the earth electrode onto the live negative electrode. The pinch chamber can be evacuated and pressurized up to 2 atm. Hydrogen is used in the experiments reported here.

The shunt resistor across the water gap enables operation of the pinch with a preheat current. Its value is chosen so that, during the pulse charging from the Marx bank, the transfer line is charged to a

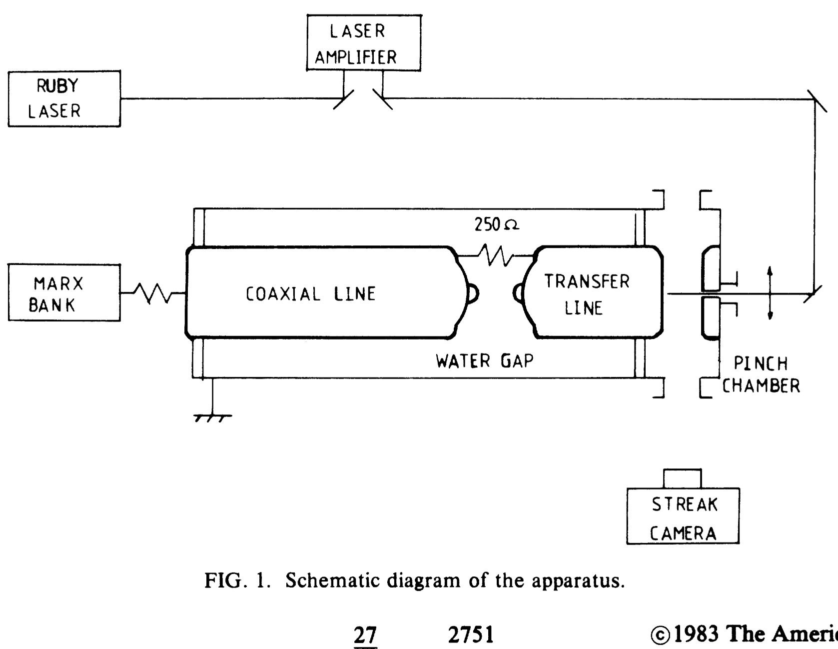

FIG. 1. Schematic diagram of the apparatus.

voltage of one-tenth that of the coaxial line. Thus, when the laser is fired, a predischarge, powered by the transfer line acting as a capacitor, is initiated between the electrodes. The predischarge has a ringing period of 80 ns and a maximum current of 6 kA. The water gap is adjusted to overvolt during the predischarge such that the main current, produced by discharge of the coaxial line, begins near the end of the first half-cycle of the predischarge. A main current of up to 50 kA with a maximum $\dot{I}$ or 5×10^{12} A s^{-1} can be generated.

The condition necessary to maintain the pinch in radial equilibrium, derived in Refs. 1–3, can be obtained more directly from the energy and pressure balance equations if we assume that, during the time under consideration, radiation and conduction losses have not yet become significant. Thus the energy balance after integration over the pinch cross section can be written as

$$\frac{d}{dt}\left(\tfrac{3}{2}\times 2NkT\right)=\frac{\eta}{\pi a^2}I^2 \ , \tag{1}$$

which equates the rate of increase of the plasma energy to the Joule heating. Here k is the Boltzmann constant, N is the electron or ion line density $(Z=1)$, T is the temperature taken to be the same for electrons and ions, I is the current which is assumed to flow uniformly over the cross section of the pinch, a is the radius, and η is the Spitzer transverse resistivity. For pressure balance, we use the Bennett relation

$$\mu_0 I^2 = 16\pi NkT \ . \tag{2}$$

Differentiating (2) and combining with Eq. (1), we obtain

$$\dot{I}=5.5\times10^{-4}\ln\Lambda\frac{N^{1/2}}{a^2T} \ , \tag{3}$$

where T is in eV. This equation specifies the value of $\dot{I}$ required to ensure that the magnetic pressure increases at the same rate as the increase in the kinetic pressure due to Joule heating. The condition for radial equilibrium derived by Manheimer[2] reduces to an identical expression if radiation and conduction losses are ignored. Assuming initial plasma conditions of $T=1$ eV, $N=3\times10^{18}$ m^{-1}, $a=10^{-4}$ m corresponding to operation at 1 atm, Eq. (3) gives $\dot{I}=3.4\times10^{14}$ A s^{-1}, which is much larger than the available $\dot{I}$. With a preheat current we may expect both a and T to be increased and thus the required $\dot{I}$ reduced.

Figure 2 shows typical streak photographs taken transversely of the pinch with and without preheat. Without preheat the pinch is seen to expand continuously; with preheat, the pinch has a constant-radius phase. The luminosity before the constant-radius phase corresponds to the preheat discharge. Similar results are obtained over the whole pressure range (0.2 to 2 atm) investigated. The constant-radius phase has duration of 40–50 ns at the low pressure and 5 ns at the high pressure. Schlieren observations of the discharge give a column radius which is identical to that obtained from the streak photographs. These observations are limited to the discharge at 1-atm hydrogen with preheat, and without preheat to the whole pressure range.

Assuming that during this time the pinch is governed by the equilibrium Eqs. (1) and (2), we may rewrite the equations to

$$T=36.1\left(\ln\Lambda\frac{I}{\dot{I}a^2}\right)^{2/3} , \quad N=1.6\times10^{11}I^2/T \ ,$$

from which T and N may be inferred taking I and $\dot{I}$ from the current waveforms and a from the streak

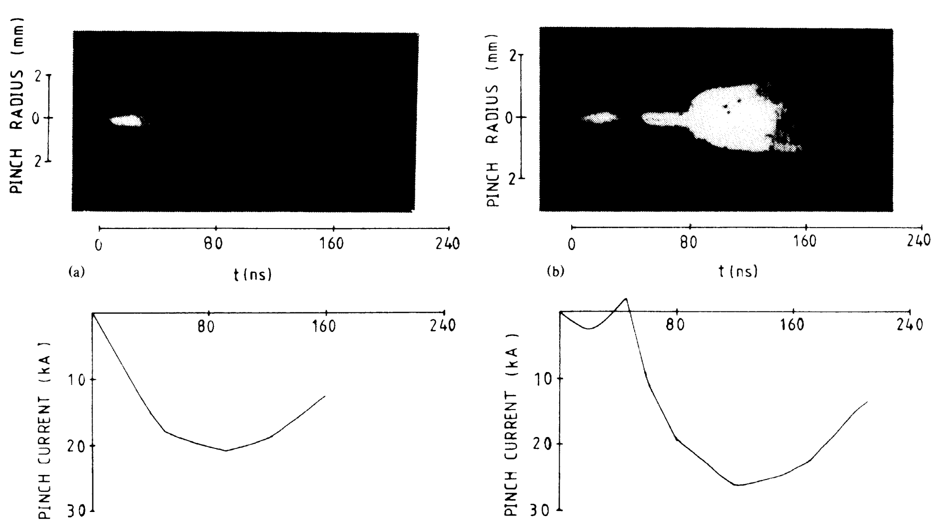

FIG. 2. Streak photographs and current wave forms at 0.33 atm in hydrogen (a) without preheat and (b) with preheat.

TABLE I. Plasma parameters calculated at the end of the constant-radius phase.

P (atm)	a (mm)	T (eV)	N (10^{18} m^{-1})	n (10^{18} cm^{-3})
0.20	0.38	52.3	1.0	2.1
0.33	0.45	34.6	1.8	2.8
1.00	0.40	19.4	3.2	6.4
1.70	0.45	16.2	3.8	6.1

photographs. Some values calculated at the end of the constant-radius phase are given in Table I. The inferred plasma parameters indicate a short electron-ion equilibration time and a current penetration depth of the order of the column radius in agreement with the assumptions made in writing Eq. (1). The table shows that the temperature decreases with pressure, which is as expected. The calculated density, however, is less than the initial density by a factor ranging from 3 at 0.2 atm to 9 at 1.7 atm. The lower density is probably due to the main pinch being formed in the rarefied core of the expanded decaying preheat discharge. This is supported by the streak photographs which show that there is an expansion of the preheat discharge. At the beginning of the main current the photographs do not show any implosion; instead, the column expands from a narrow filamentary discharge to its equilibrium radius in a time <5 ns.

The expansion seen in the streak photographs in

(a)

(b)

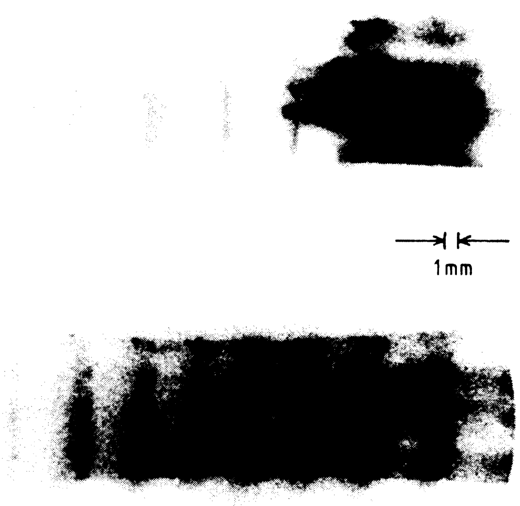

FIG. 3. Framing camera photographs at 0.33 atm in hydrogen. Time between frames is (a) 13.3 ns in the upper sequence and (b) 3.3 ns in the lower sequence.

Fig. 2 at the end of the constant-radius phase is, in fact, associated with the transformation of the pinch into a helix which then expands radially. This can be seen in Fig. 3 which shows a typical sequence of framing photographs. The top sequence shows the preheated column followed by the narrower pinch with constant radius and then the transition to a helical structure. The lower sequence shows the radial expansion of the helical structure with a better time resolution. At higher pressures the structure is less well defined. The rapid transition to a helix and the subsequent radial expansion constitute a large rate of change of inductance $\dot{L}$ and hence a large "dynamic resistance" in the circuit. Estimates of the value of $\dot{L}$ indicate that it may easily exceed the line impedance. This possibly accounts for the different current waveforms observed at different gas pressures.

The observed characteristics of the helical instability appear to be in good agreement with the calculations of Felber and Rostocker[6] for the magnetohydrodynamic $m=1$ instability. At 0.33 atm the ratio of the pitch of the helix to the column radius is observed to be 4.6. The theoretical prediction for the fastest growing modes is $\lambda/a=4$, where λ is the wavelength and a is the radius. The growth time obtained by calculating $r/\dot{r}$ from the streak photographs immediately after the constant current phase increases with pressure being 10 ns at 0.2 atm and 15 ns at 1.7 atm. The theoretical values are 3.5 ns at the low pressure and 7.4 ns at the high pressure. The discontinuity in the expansion seen in the streak photographs is presumably due to the onset of nonlinearity and occurs at $r/a \sim 3.36 \pm 0.01$ (averaged over all shots over the whole pressure range), where r is the major radius of the helix. Nonlinear behavior is predicted when the perturbation amplitude becomes equal to $4a$.

It is of interest to note that stabilization due to finite Larmor radius is predicted for the $m=0$ mode in the Z pinch[7] and for all modes in the θ pinch.[8,9] In our experiment the ratio of the ion Larmor radius to the pinch radius is >0.1, but $\omega\tau<1$ for the ions. Stabilization due to the surrounding gas predicted by Manheimer *et al.*[10] is presumably not occurring due to the low density of the surrounding gas caused by the preheat discharge.

*Permanent address: Department of Physics, Universiti Malaya, Kuala Lumpur, Malaysia.

[1]M. G. Haines, Proc. Phys. Soc. London 76, 250 (1960).
[2]W. M. Manheimer, Phys. Fluids 17, 1767 (1974).
[3]H. W. Bloomberg, M. Lampe, and D. G. Colombant, J. Appl. Phys. 51, 5277 (1980).
[4]L. A. Jones, K. H. Finken, A. E. Dangor, E. Källne, S. Singer, I. R. Lindemuth, J. H. Brownell, and T. A. Oliphant, Appl. Phys. Lett. 38, 522 (1981).
[5]E. A. Smärs, Ark. Fys. 29, 97 (1964).
[6]F. S. Felber and N. Rostocker, Phys. Fluids 24, 1049 (1981).
[7]D. E. Potter, Phys. Fluids 14, 1911 (1971).
[8]E. Bowers and M. G. Haines, Phys. Fluids 14, 165 (1971).
[9]J. P. Freidberg, Phys. Fluids 15, 1102 (1972).
[10]W. M. Manheimer, M. Lampe, and J. P. Boris, Phys. Fluids 16, 1126 (1973).

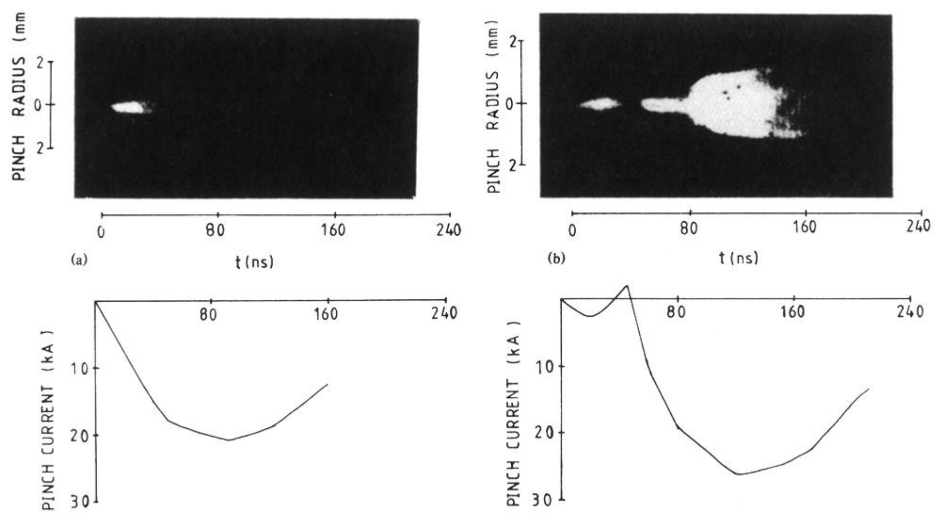

FIG. 2. Streak photographs and current wave forms at 0.33 atm in hydrogen (a) without preheat and (b) with preheat.

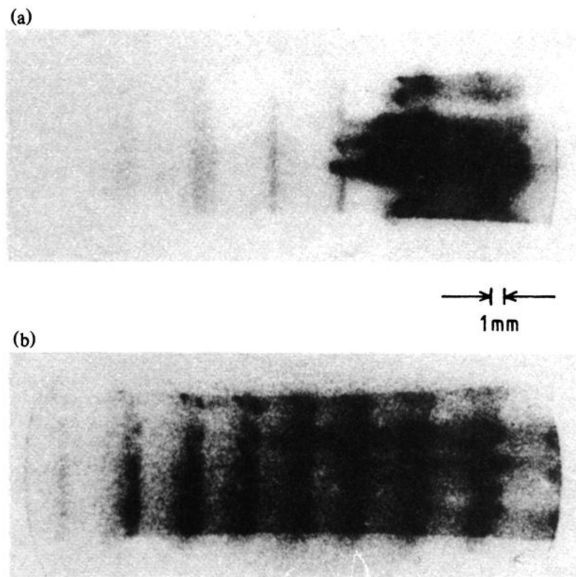

FIG. 3. Framing camera photographs at 0.33 atm in hydrogen. Time between frames is (a) 13.3 ns in the upper sequence and (b) 3.3 ns in the lower sequence.